Biophysical Journal, Volume *116*

Supplemental Information

Structure and Conformation of Wild-Type Bacterial Lipopolysaccharide Layers at Air-Water Interfaces

Samantha Micciulla, Yuri Gerelli, and Emanuel Schneck

Supporting Information for "Structure and conformation of wild-type bacterial lipopolysaccharide monolayers at air/water interfaces"

S. Micciulla, Y. Gerelli, E. Schneck

Wild-type LPS monolayer stability on Ca^{2+}-free subphase

Figure S1a shows the pressure versus area isotherms for subsequent compression/expansion cycles of a wild-type LPS monolayer spread onto *Ca^{2+}-free* subphase. Similar to the behavior of this monolayer onto *Ca^{2+}-loaded* subphase reported in the manuscript, there is a clear evidence of hysteresis at each cycle, with a relative reduction of the specific area at the highest pressure (π = 45 mN/M) per cycle between ≈ 3% and ≈ 8%.

As for *Ca^{2+}-loaded* LPS, the kinetics of the area reduction shows a dependence on the applied lateral pressure (Figure S1b and c): at an initial pressure of π = 15 mN/m and constant surface area, the pressure decreases with $d\Pi/dt \approx 0.04$ mN/(m min), while for initial π = 30 mN/m, the pressure decreases about four times as fast ($d\Pi/dt \approx 0.16$ mN/(m min)).

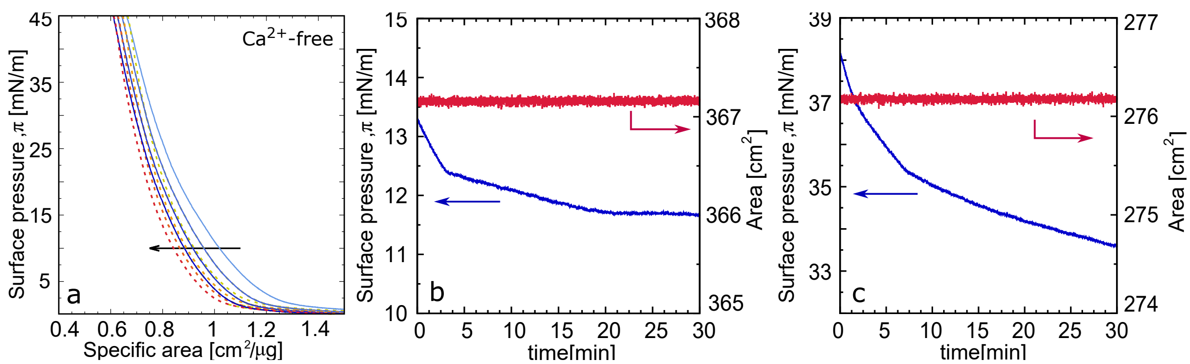

Figure S1: (a): Repeating compression cycles of wild-type LPS monolayers on *Ca^{2+}-free* subphase. (b, c): Evolution of surface pressure over time at constant area starting with an initial surface pressure of about 15 mN/m (b) and about 30 mN/m (c).

Table S1: Best-fit parameters obtained from the analysis of the reflectivity data. The roughness σ for the HC refers to the air/HC interface, while the value for IOS refers to the IOS/water interface. The symbols *n,x* indicate the different contrasts (neutron and X-ray); the symbols *f,l* represent the *free* and *loaded* subphase, respectively.

Parameter	HC	IOS	OSC
$\rho_{i,f}^{n,D_2O}$ [Å^{-2}]	0.4 x 10^{-6}	2.60 x 10^{-6}	2.16 x 10^{-6}
$\rho_{i,l}^{n,D_2O}$ [Å^{-2}]	0.4 x 10^{-6}	2.56 x 10^{-6}	2.12 x 10^{-6}
$\rho_{i,f}^{n,ACMW}$ [Å^{-2}]	0.4 x 10^{-6}	-0.041 x 10^{-6}	-0.034 x 10^{-6}
$\rho_{i,l}^{n,ACMW}$ [Å^{-2}]	0.4 x 10^{-6}	-0.139 x 10^{-6}	-0.011 x 10^{-6}
ρ_i^x [Å^{-2}]	8.0x 10^{-6}	15.2 x 10^{-6}	14.2 x 10^{-6}
d_f [Å]	20 (1)	20 (1)	-
d_l [Å]	15 (1)	17 (2)	-
λ_f [Å]	-	-	119 (10)
λ_l [Å]	-	-	130 (10)
n_f	-	-	1.4 (0.1)
n_l	-	-	1.3 (0.1)
σ_f [Å]	3 (1)	7 (2)	-
σ_l [Å]	3 (1)	14 (2)	-